



Effect of heat treatment on the structure and creep resistance of austenitic Fe–Ni alloy

K.J. Ducki*

Materials Science Department, Silesian University of Technology,
ul. Krasińskiego 8, 40-019 Katowice, Poland

* Corresponding author: E-mail address: kazimierz.ducki@polsl.pl

Received 28.11.2010; published in revised form 01.01.2011

ABSTRACT

Purpose: The paper addresses the problem of determining the dependence between the initial heat treatment of an austenitic Fe–Ni alloy and its structure, and its creep resistance. Specimens of Fe–Ni alloy were subjected to tests after two variants of heat treatment, i.e. solution heat treatment followed by typical single-stage ageing, and solution heat treatment followed by novel two-stage ageing.

Design/methodology/approach: For the investigated Fe–Ni alloy after solution heat treatment in the conditions: 980°C/2h/water, two variants of specimen ageing were applied for a comparison: single-stage ageing (715°C/16h/air) and two-stage ageing (720°C/8h + cooling in the furnace up to the temperature of 650°C + 650°C/8h/air). The thermally treated specimens were then subjected to a static tensile test at room and elevated temperatures, and to a creep test in a temperature range of 650–750°C, at stresses from 70 to 340 MPa.

Findings: It was found that both, at the room and elevated temperatures, the specimens of Fe–Ni alloy after 2-stage ageing were distinguished by higher strength properties (Y.S, T.S) with a little lower plastic properties (EL., R.A). As regards extrapolated results of creep tests, it was found that at a longer exposure time of ca. 10.000 h, specimens after single-stage ageing were characterized with higher creep resistance. Lower creep resistance of the Fe–Ni alloy after two-stage ageing can be explained by increased brittleness of the material in boundary areas.

Practical implications: The obtained test results may be used to optimise heat treatment and forecast the operation conditions of products made out of Fe–Ni alloy at an elevated temperature.

Originality/value: The study shows a significant effect of the applied ageing variants on mechanical properties and creep resistance of the tested austenitic Fe–Ni alloy.

Keywords: Creep resistance; Metallic alloys; Heat treatment; Structure

Reference to this paper should be given in the following way:

K.J. Ducki, Effect of heat treatment on the structure and creep resistance of austenitic Fe–Ni alloy, Archives of Materials Science and Engineering 47/1 (2011) 33–40.

PROPERTIES

1. Introduction

Austenitic Fe–Ni alloys precipitation-strengthened with intermetallic phases of type γ' [$\text{Ni}_3(\text{Al,Ti})$] are characterised by various characteristic properties, such as [1-6]: high mechanical properties, considerable creep resistance and heat resistance at slightly elevated and high temperatures, excellent corrosion resistance, high ductility at low temperatures, and are non-magnetic. The temperature range, within which these alloys can be used, spreads from the temperature of liquid helium (-269°C) up to temperature within a range of $540\text{--}815^\circ\text{C}$. This modern group of metallic materials is more and more widely utilised in the conventional power industry and nuclear power engineering, aeronautical engineering, chemical and petrochemical industry, cryogenic engineering and for tools in nonferrous metals processing.

High-temperature Fe–Ni alloys obtain their optimum properties after multi-stage heat treatment consisting of solution heat treatment (or annealing) and various ageing variants. Most frequently for such type of alloys, solution heat treatment from a temperature of circa 1000°C in water or oil and ageing at temperature of $710\text{--}730^\circ\text{C}$ during 16–20 h with subsequent cooling in the air are applied [7-10]. For some Fe–Ni alloys (for instance Inconel 706 and 901) after solution heat treatment, it is recommended to apply two-stage ageing, which consists of carrying out a controlled cooling cycle between two isothermal soaking processes [11-14]. Such processing is aimed at obtaining optimum values and distribution of precipitates of the γ' type intermetallic phase, which ensures maximum strength coupled with good alloy plasticity under creep conditions at a temperature of $650\text{--}700^\circ\text{C}$.

In the presented paper, investigation was initiated concerning the effect of initial heat treatment on the structure, mechanical properties and creep resistance of an austenitic Fe–Ni alloy precipitation-strengthened with an intermetallic phase of the γ' type. Specimens of Fe–Ni alloy were subject to tests after two variants of heat treatment, i.e. solution heat treatment followed by typical single-stage ageing, and solution heat treatment followed by novel two-stage ageing. The paper constitutes continuation of the research [15-19] on the structure and properties of austenitic Fe–Ni alloys precipitation-strengthened with intermetallic phases.

2. Material and procedure

The examinations were performed on rolled bars, 16 mm in diameter, of an austenitic Fe–Ni alloy of A-286 type. The chemical composition of the material is given in Table 1.

Specimens of Fe–Ni alloy were subjected to tests after two variants of heat treatment, i.e. solution heat treatment and single-stage ageing (variant A) and solution heat treatment followed by two-stage ageing (variant B). Parameters of heat treatment for the investigated Fe–Ni alloy were determined based on the previously carried out studies [15, 19] and data from professional literature

[7-10]. For the investigated alloy after solution heat treatment in the conditions: $980^\circ\text{C}/2\text{h}/\text{water}$, two variants of specimens' ageing were used for comparison, i.e.:

- single-stage ageing (variant A): $715^\circ\text{C}/16\text{h}/\text{air}$;
- two-stage ageing (variant B): $720^\circ\text{C}/8\text{h}$ + cooling in the furnace up to a temperature of 650°C + $650^\circ\text{C}/8\text{h}/\text{air}$.

A schematic course of heat treatment of specimens made of the investigated alloy is presented in Fig. 1.

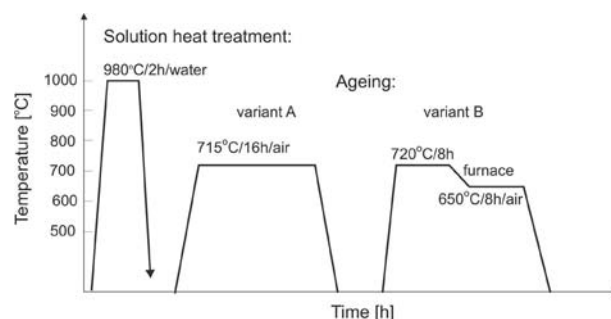


Fig. 1. Diagram of heat treatment of specimens of A and B variants of the investigated Fe–Ni alloy

A static tensile test was carried out using a strength testing machine MTS-810. The examinations were carried out at room temperature and at an elevated temperature in the range of $600\text{--}750^\circ\text{C}$. Cylindrical five-time specimens with a diameter $d_0 = 10$ mm and measuring length $l_0 = 50$ mm were used for the tests. A conventional yield point (Y.S), tensile strength (T.S), unit elongation (EL.) and reduction of area (R.A) were determined.

Shortened creep tests of specimens made of the investigated Fe–Ni alloy were conducted in the creep laboratory of The Institute for Ferrous Metallurgy in Gliwice. The tests were performed in compliance with standard PN-76/H-04330 in a temperature range of $650\text{--}750^\circ\text{C}$ and at stresses between 70 and 340 MPa. The tests were carried out in single-specimen six-stand testing machines of maximum load of 50 kN, adjusted to measure elongation during the test. Specimens with diameter $d_0 = 5$ mm and measuring length $l_0 = 50$ mm were used for creep tests (their measuring length was 10 times bigger than diameter).

The tests were carried out until specimen failure (in the time range from 60 to 1301 h) and elongation of the specimen was measured during the test. After failure, the final elongation and reduction of area of the specimen were measured at room temperature. For cognitive and comparative purposes, creep tests were conducted on alloy specimens after solution heat treatment and single-stage ageing (variant A), and after solution heat treatment followed by two-stage ageing (variant B). Specimens of variant A for the creep tests were marked with subsequent numbers A1-A9, whereas specimens of variant B, with subsequent numbers B1-B9. Detailed data regarding the method of marking the specimens of Variants A and B and the parameters of creep tests conducted for particular specimens are provided in Table 3.

Table 1.

Chemical composition of the investigated Fe–Ni austenitic alloy

Content of an element, wt. %															
C	Si	Mn	P	S	Cr	Ni	Mo	V	W	Ti	Al	Co	B	N	Fe
0.05	0.55	1.25	0.026	0.016	14.3	24.5	1.34	0.41	0.10	1.88	0.16	0.08	0.007	0.0062	55.32

Specimens structural tests were conducted on a Reichert MeF-2 light microscope. The surface of specimens with diameters of 10 and 12 mm was initially ground on a disc grinder and next, on waterproof abrasive papers with graining of 80-2000. Final surface processing consisted of polishing with diamond paste on a semi-automatic Struers grinding machine. The specimens were etched using a reagent with the following composition: 54 cm³ of hydrofluoric acid (HF), 8 cm³ of nitric acid (HNO₃) and 38 cm³ of distilled water.

Tests of the specimens' substructure were carried out using a thin foil technique on a Jeol transmission electron microscope, JEM-2000 FX, at accelerating voltage of 160 kV. The discs for thin foils with a diameter of 3.0 mm and thickness of about 0.5 mm were cut out from a previously prepared shaft, 3.0 mm in diameter, by means of a Struers cutting-off machine, Acutom. The discs were initially ground with waterproof abrasive papers until the thickness of ca. 0.05 mm was obtained. The so obtained discs were then thinned via two-sided jet electrolytic polishing method in a Tenupol-3 device of Struers manufacture. A company brand reader A-8 was used (for alloys with a Fe matrix) cooled down to a temperature 15°C at polishing voltage of 80 V.

Fractographic tests fractures of specimens after creep were carried out on a Jeol JSM-35 scanning microscope. Structural observations were conducted on fractures drawn from the specimens after creep. The purpose of fractographic tests was to evaluate the nature of fractures which formed on the specimens during creep and to analyze plastic properties of the material after both variants of heat treatment.

3. Experimental results

The results of specimens' microscope observations of the Fe–Ni alloy after both variants of heat treatment are presented in Figs. 2 and 3. In both cases, the initial alloy microstructure demonstrated an austenitic matrix with a diversified grain size and with numerous twin systems as well as particles of primary and secondary precipitates.

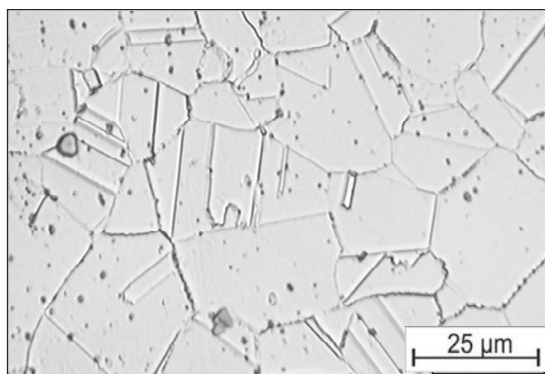


Fig. 2. Alloy structure after solution heat treatment and ageing according to variant A. Austenite with a diversified grain size, with primary and secondary precipitates

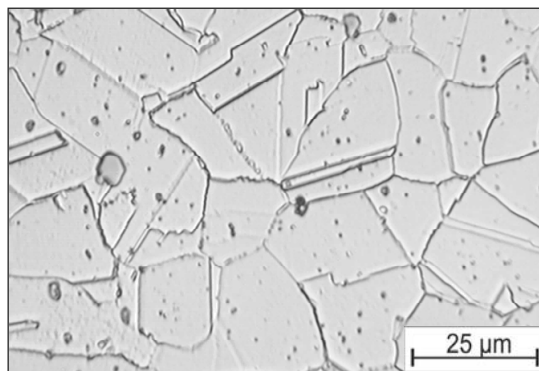


Fig. 3. Alloy structure after solution heat treatment and ageing according to variant B. Austenite with a diversified grain size, with primary and secondary precipitates

By comparing both of the Fe–Ni alloy structures, it can be assumed that in the alloy after 2-stage ageing (variant B), a higher fraction of secondary phase particle precipitates is observed on grain boundaries in relation to 1-stage ageing (variant A).

This finding is corroborated by the results of research on the Fe–Ni alloy substructure conducted using a transmission electron microscope (Figs. 4 and 5). It has been found that the precipitation process in the alloy substructure for variant A took place mainly within the matrix, where a characteristic “tweed-like” contrast connected with the occurrence of coherent particles of the intermetallic phase type γ' [$\text{Ni}_3(\text{Al,Ti})$] was identified (Fig. 4). As for variant B, the precipitation process of secondary phase particles took place both within the matrix and along the grain boundaries (Fig. 5). Early stages of type γ' phase precipitates were observed in the matrix, whereas within the area of grain boundaries, the occurrence of M_{23}C_6 carbide lamellae and lenticular particles of the G [$\text{Ni}_{16}\text{Ti}_6\text{Si}_7$] intermetallic phase [10] were observed.

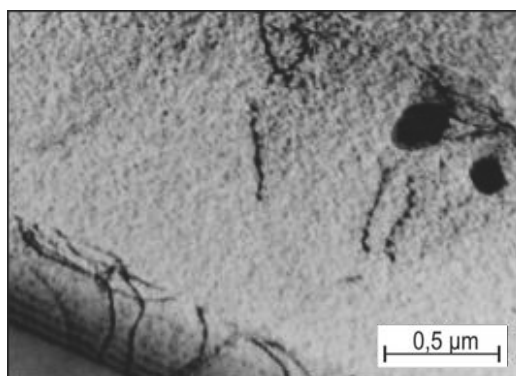


Fig. 4. Alloy substructure after heat treatment according to variant A. Coherent precipitates of phase γ' and lenticular particles of phase G in the matrix

The static tensile test conducted on Fe–Ni alloy specimens at room and elevated temperatures were supplement to the creep test conducted in parallel. For cognitive and comparative purposes, the tests were conducted on alloy specimens after solution heat treatment and single-stage ageing (variant A), and after solution

heat treatment followed by two-stage ageing (variant B). The obtained results of tests of mechanical properties of the Fe-Ni alloy at room and elevated temperatures are presented in Table 2.

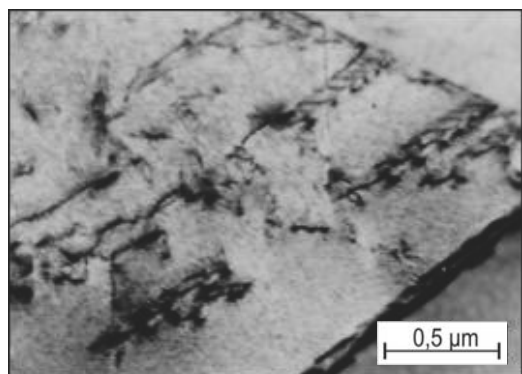


Fig. 5. Alloy substructure after heat treatment according to variant B. Coherent precipitates of phase γ' in the matrix and $M_{23}C_6$ carbide lamellae, and phase G particles on grain boundary

Table 2. Mechanical properties of the Fe-Ni alloy after ageing according to variants A and B at room and elevated temperatures

Variant of ageing	Test temperature [°C]	Y.S [MPa]	T.S [MPa]	EL. [%]	R.A [%]
A	20	701	1021	27	48
B		761	1097	26	46
A	600	632	802	12	39
B		698	879	11	37
A	650	611	708	11	29
B		639	762	10	25
A	700	513	560	10	38
B		473	531	10	35
A	750	363	421	27	59
B		368	433	22	54

Based on the provided results of tests at room temperature (20°C), it can be seen that specimens of variant B, i.e. those after 2-stage ageing, demonstrated better strength properties (Y.S = 761 MPa, T.S = 1097 MPa). Specimens of variant A (after 1-stage ageing) demonstrated a little worse strength properties (Y.S = 702 MPa, T.S = 1021 MPa) with their plastic properties being comparable.

Also, tests at elevated temperature, in the range of 600-750°C, showed that specimens of variant B (Table 2) were characterized with better strength properties (Y.S= 699 -368 MPa, T.S=879-433 MPa), with their plastic properties being a little worse (EL. = 10-22.2%). Specimens of variant A in an analogical range of test temperatures demonstrated a little worse strength properties (Y.S= 632-363 MPa, T.S = 802-421 MPa) with their plastic properties being a little higher (EL.= 10.2-27.2%).

Based on the test results obtained, it is possible to affirm that specimens made of the examined alloy subjected to 2-stage ageing (variant B) were characterized with stronger strengthening at both room and elevated temperatures. In turn, specimens of the examined alloy subjected to 1-stage ageing (variant A) were characterized with a little higher plasticity at room temperature and at elevated temperatures. Higher strength-related properties

with the slightly lower plastic properties of the specimens after 2-stage ageing can be accounted for by stronger strengthening of grain boundaries and the zones near boundaries through precipitation of $M_{23}C_6$ carbides and phase G [$Ni_{16}Ti_6Si_7$] [10].

Results of shortened creep tests of specimens of variants A and B at temperatures from the range of 650-800°C and stress of 70-340 MPa are given in Table 3. They are also presented in a form of cumulative creep curves in consecutive Figs. 6-8. It appears from the diagrams obtained that all creep curves have a shape characteristic of the accelerated creep stage. For a given test temperature, the shape of creep curves significantly depends on the value of the stress applied. A comparison of the alloy creep curves at a temperature of 650°C gave quite diversified results, depending on the value of the stress applied (Fig. 6). At high stresses, i.e. 340 and 260 MPa, specimens of variant B demonstrated a slower deformation rate, whereas at a lower stress (240 MPa), specimens of variant A showed a slower deformation rate.

Table 3. Specification of specimens and results of shortened creep tests of the Fe-Ni alloy after ageing for variants A and B

Sign of sample	Temp. [°C]	Stress [MPa]	Time to rupture [h]	EL. [%]	R.A. [%]
A1	650	340	70	6	30
B1	650	340	132	5	28
A2	650	260	649	9	28
B2	650	260	709	7	11
A3	650	240	1014	7	15
B3	650	240	1025	7	16
A4	700	240	60	15	20
B4	700	240	99	15	19
A5	700	180	941	22	43
B5	700	180	1009	15	36
A6	700	150	1186	21	39
B6	700	150	1165	22	42
A7	750	120	120	28	73
B7	750	120	170	28	75
A8	750	80	789	33	77
B8	750	80	692	35	42
A9	750	70	1284	27	48
B9	750	70	1301	32	54

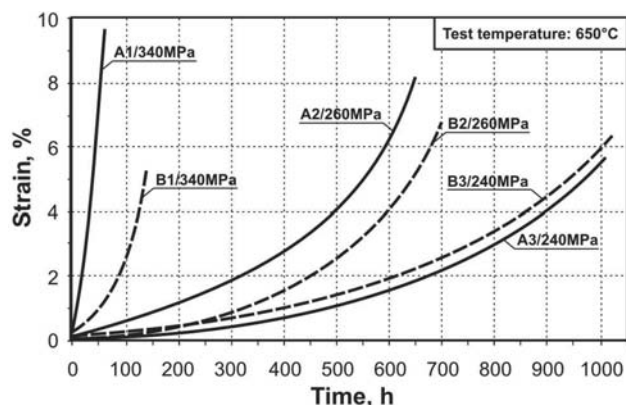


Fig. 6. Comparison of creep curves of specimens of variants A and B at a temperature 650°C and stresses: 340, 260 and 240 MPa

At a higher test temperature, 700°C, a similar diversity of results concerning the creep resistance was obtained (Fig. 7). At higher stresses, of 240 and 180 MPa, specimens of variant B demonstrated a lower deformation rate. In turn, at a lower stress (150 MPa), specimens of variant A showed better creep resistance.

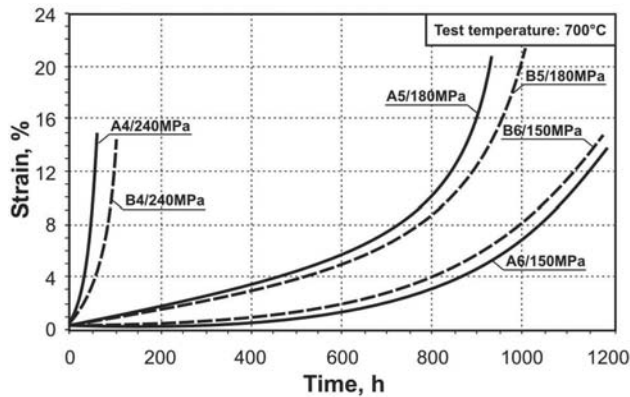


Fig. 7. Comparison of creep curves of specimens of variants A and B at a temperature 700°C and stresses: 240, 180 and 150 MPa

A comparison of creep curves for the alloy at the highest tested temperature, i.e. 750°C, also yields diversified results, depending on the value of the stress applied (Fig. 8). At high stresses ($\sigma = 120$ MPa), a specimen of variant B demonstrated a slower deformation rate, whereas at a lower stress ($\sigma = 80$ MPa), a specimen of variant A showed a slower deformation rate. At the lowest stress ($\sigma = 70$ MPa), the deformation rates for specimens of variants A and B were similar.

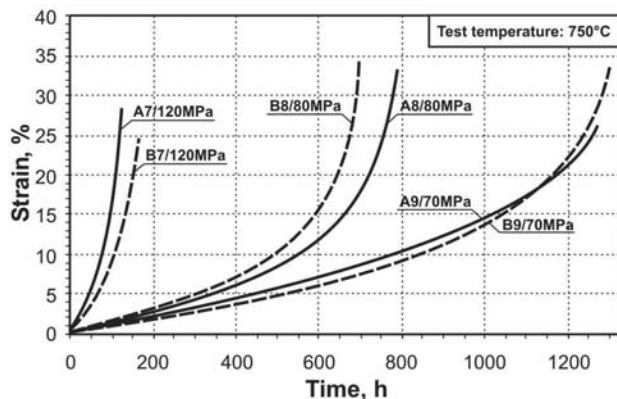


Fig. 8. Comparison of creep curves of specimens of variants A and B at a temperature 700°C and stresses: 240, 180 and 150 MPa

Based on the obtained shortened creep curves of specimens of the tested Fe–Ni alloy, the creep test results were then extrapolated. The extrapolation was performed using a graphical method [20] for creep times equal 100, 1000 and 10000 h, at the examined test temperatures of 650, 700 and 750°C. Results of extrapolation of the creep tests for variants A and B are given in Table 4 and presented graphically in Fig. 9. As can be seen from

the results obtained, at the lowest creep temperature of 650°C and in the range of short and medium test time of 100 -1000 h, higher creep resistance was exhibited by specimens of variant B. In turn, at the longest analysed creep time – 10000 h – specimens of variant A demonstrated better temporal strength. At higher test temperature of 700°C and short creep time of 100 h, specimens of variant B demonstrated higher creep resistance. In turn, at longer test time of 1000-10.000 h, specimens treated thermally according to variant A demonstrated better temporal strength.

Table 4.

Extrapolated values of temporal creep strength of specimens of variant A and B of Fe–Ni alloy for test time 100, 1000 and 10000 h

Time of test creep [h]	Creep strength [MPa] at temperature:					
	650°C		700°C		750°C	
	Variant A	Variant B	Variant A	Variant B	Variant A	Variant B
100	327	353	226	239	124	132
1000	242	245	167	150	75	74
10000	157	138	109	61	27	16

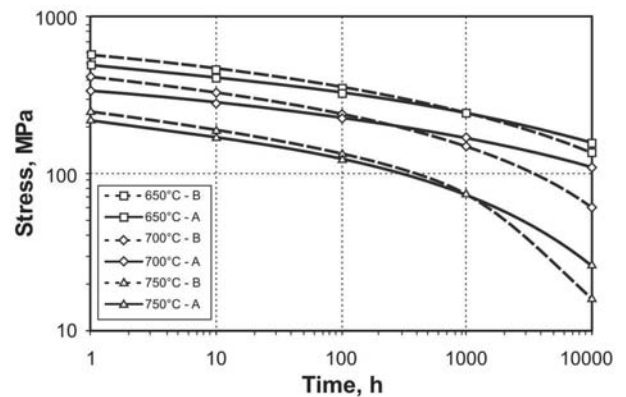


Fig. 9. Extrapolation of creep test results at the temperature of 650, 700 and 750°C for specimens of Fe–Ni alloy after ageing according to variants A and B

Also at the highest test temperature of 750°C and short creep time of 100 h, specimens of variant B demonstrated higher creep resistance. At the average test time of 1.000 h, specimens of variants A and B obtained similar temporal strengths. At the longest analysed creep time – 10.000 h – specimens of variant A reached significantly higher creep resistance in comparison with specimens of variant B.

Structural examination with use of transmission electron microscope (TEM) was performed with thin foil technique. Specimens for thin foils were drawn transversely from the part adjacent to the fractures created during creep. The purpose of the tests was to reveal changes in the alloy substructure, formed during creep. The results of tests for the selected specimens after creep are presented in Figs. 10-12. In the substructure of specimens subject to creep at the temperature of 650°C and stress $\sigma = 240$ MPa, dislocation clusters were revealed in boundary areas. Inside the matrix grains, effects of blocking the dislocation motion by dispersive γ' phase particles (Fig. 10) were observed. Presence of such effects in the alloy substructure shows that creep at the temperature of 650°C is of dislocation nature.

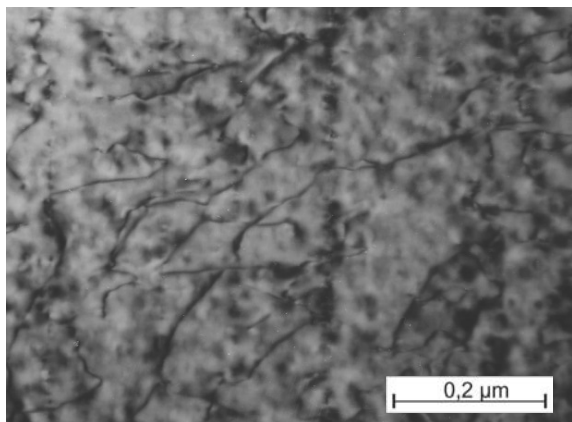


Fig. 10. Substructure of B3 specimen after creep test 650°C/240 MPa. Blocking the dislocation motion by dispersive γ' phase particles in the matrix

In the substructure of specimens subject to creep at the temperature of 700°C and stress $\sigma = 150$ MPa, a significantly larger density of dislocation clusters in matrix was revealed. In the boundary areas of the matrix, advanced stages of recovery and of coagulation of γ' phase particles were observed as well as deformation of some primary precipitates by formation of internal stacking faults (Fig. 11). Revealing this type of substructure in the specimens analyzed shows that creep at the temperature of 700°C is of complex nature which may be defined as dislocation-diffusive.

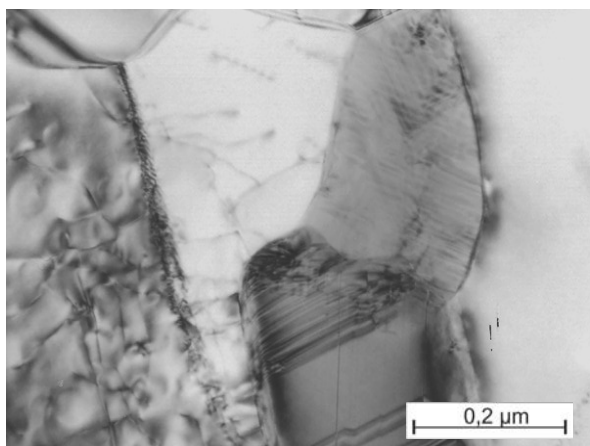


Fig. 11. Substructure of B6 specimen after creep test 700°C/150 MPa. Processes of matrix recovery, γ' particles coagulation and deformation of primary precipitates

In the substructure of specimens subjected to creep at the temperature of 750°C and stress $\sigma = 70$ MPa, areas of diverse dislocation density were detected, as well as clearly noticeable effects of overageing of the alloy connected with the $\gamma' \rightarrow \eta$ transformation (Fig. 12). The formation of a number of transcrystalline and cellular η phase lamellae was accompanied with dissolution of the neighbouring γ' phase particles and decrease of dislocation

density in the matrix. Presence of such effects in the alloy substructure shows that creep at the temperature of 750°C is mainly of diffusive nature.

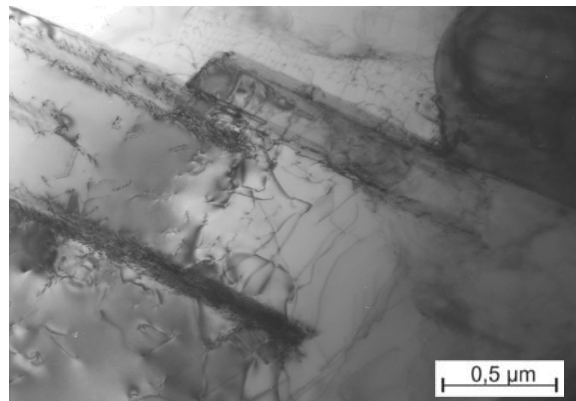


Fig. 12. Substructure of A9 specimen after creep test 750°C/70 MPa. Transcrystalline lamellae of phase η in the matrix of low dislocation density

Fractographic tests were conducted on fractures drawn from selected specimens after creep. The purpose of the tests was to evaluate the nature of fractures formed in the specimens during creep. The results of the fractographic tests of specimens of variants A and B after creep are presented in Figs. 13-15. In the specimens subject to creep at the temperature of 650°C and stress of 240 MPa, a predominant fraction of ductile fracture with a minor fraction of brittle intergranular cracks was revealed (Fig. 13). Specimen of variant B, i.e. after two-stage ageing, was characterized with a more cleavable nature, with a larger fraction of intergranular cracks.

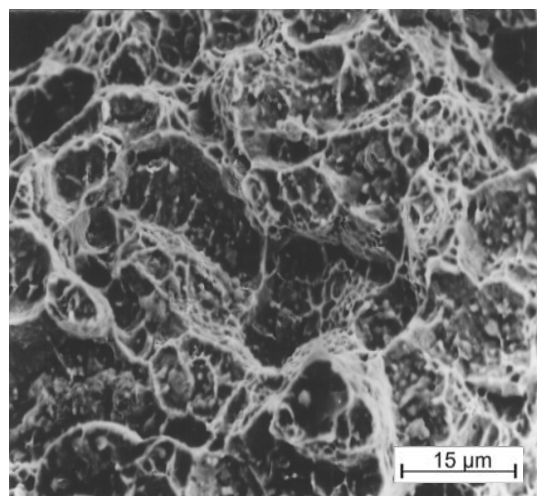


Fig. 13. Fracture of B3 specimen after creep test 650°C/240 MPa. Ductile fracture with larger fraction of cleavage cracks

A similar type of ductile fracture with a little larger fraction of intergranular cleavage cracks was observed in specimens after creep at the temperature of 700°C and stress of 150 MPa (Fig. 14). Also in this case, a specimen treated thermally according to variant B, i.e. after 2-stage ageing, was characterized with a little higher fraction of brittle cracks.

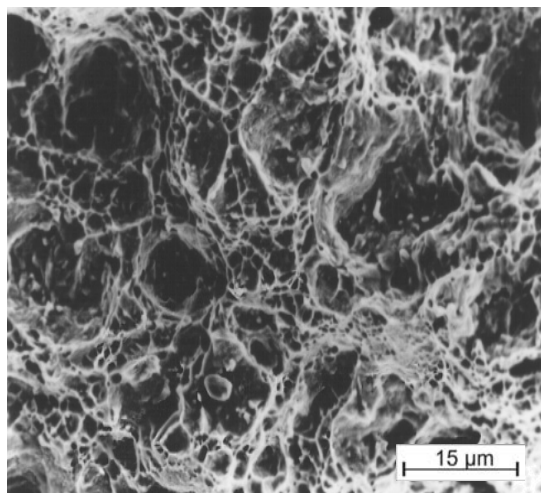


Fig. 14. Fracture of A6 specimen after creep test 700°C/150 MPa. Ductile fracture with small fraction of cleavage cracks

Also in the specimens after creep at the highest temperature of 750°C and stress of 70 MPa, a predominant fraction of ductile fracture with some fraction of cleavage cracks was revealed (Fig. 15).

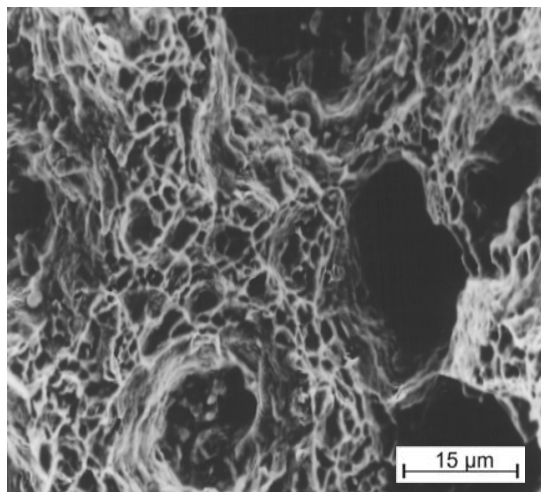


Fig. 15. Fracture of B9 specimen after creep test 750°C/70 MPa. Ductile fracture with fraction of cleavage cracks

In this case, on the fracture surface of both specimens tested, traces of significant oxidation were found, whereas fraction of brittle cracks for specimens of variants A and B was comparable.

4. Conclusions

The paper analyses the influence of initial thermal treatment on the structure and mechanical properties of the austenitic Fe–Ni alloy precipitation-strengthened with intermetallic phases of the γ' [$\text{Ni}_3(\text{Al,Ti})$] type. Samples of the studied alloy after solution heat treatment (980°C/2h/water) were subjected to two ageing variants, i.e. 1-stage ageing (715°C/16h/air) – variant A and 2-stage ageing (715°C/8h/furnace+650°C/8h/air) – variant B. On thermally-treated specimens according to variants A and B, static tensile tests and shortened creep tests were performed in a range of temperature of 650–750°C and at stresses from 70 to 340 MPa.

In the structure of the studied Fe–Ni alloy, for both ageing variants A and B, an austenitic matrix was detected with a diversified grain size and undissolved particles of titanium compounds, and coherent dispersion precipitates of the γ' intermetallic phase. It has been found that in the 2-stage aged alloy the precipitation process was proceeding to a greater extent along grain boundaries, where lamellar precipitates of M_{23}C_6 carbide and lenticular particles of phase G [$\text{Ni}_{16}\text{Ti}_6\text{Si}_7$] were identified. Such course of precipitation in the alloy thermally treated according to variant B can result in both, enhanced strengthening of the areas near boundaries and in material increased brittleness in those regions.

Static tensile tests of Fe–Ni alloy, conducted at the temperature of 20°C demonstrated higher strength properties of the specimens of variant B (Y.S = 761 MPa, T.S = 1097 MPa) compared to variant A (Y.S = 701 MPa, T.S = 1021 MPa), with their plastic properties being comparable. Also, at the increased temperature of 600–750°C, variant B specimens were characterized by higher strength properties (Y.S = 699–368 MPa, T.S = 879–433 MPa) in comparison with variant A (Y.S = 632–363 MPa, T.S = 802–421 MPa).

Shortened creep tests demonstrated the diversified influence of applied ageing variants A and B on the temporal strength of Fe–Ni alloy tested. It was found that in the scope of the short and medium creep time tested of ca. 100 and 1000 h at the temperature of 650–750°C, higher creep resistance was exhibited by specimens of variant B, i.e. after 2-stage ageing. In turn, extrapolation of results of creep tests to 10000 h conducted with graphical method showed that specimens of variant A, i.e. after 1-stage ageing showed higher creep resistance at the temperature of 650–750°C.

The reason for lower creep resistance of the specimens treated thermally according to variant B should be sought in a larger number of secondary phase particles precipitated on grain boundaries, which determines earlier initiation of the creep microcracks. This has been corroborated by the observation of the fractures morphology of specimens after creep where a faster development and larger fraction of intergranular cracks was found, indicating lower cohesion of the grain boundaries, especially at elevated temperature in the scope of 700–750°C.

It was found that the substructure of specimens after creep of both variants of Fe–Ni alloy ageing depends basically on the creep temperature which determines also the creep mechanism. At the temperature of 650°C, creep is mainly of dislocation nature, and in the alloy substructure, increased density of dislocation was observed in a form of clusters, the movement of which was blocked by dispersive γ' phase particles. At higher temperature of

700°C, creep is of complex, dislocation – diffusive nature, and in the alloy substructure, both the reinforcement effect and dynamic recovery effects were revealed as well as coagulation process of γ' phase particles. At the highest temperature of 750°C, creep is mainly of a diffusive nature, and in the alloy substructure, distinct effects of overageing are observed, connected with transformation $\gamma' \rightarrow \eta$, accompanied with dissolution of the neighbouring γ' phase particles and a decrease of dislocation density in the matrix.

On the basis of the results obtained, a conclusion can be drawn that the studied Fe–Ni alloy is characterized by better material characteristics after solution heat treatment and 1-stage ageing at 715°C/16h/air. With its slightly decreased strength properties, the alloy heat treated according to variant A shows definitely higher temporal creep strength, especially at the temperature within the range of 700-750°C and extended operation time of ca. 10000 h.

Acknowledgements

This scientific work was partially financed within the Research Project No 0 R00 0051 08 headed by Prof. L. Swadźba.

References

- [1] M. Konter, M. Thumann, Materials and manufacturing of advanced industrial gas turbine components, *Journal of Materials Processing Technology* 117 (2001) 386-390.
- [2] R. Shargi-Moshtaghin, S. Asgari, The influence of thermal exposure on the γ' precipitates characteristics and tensile of superalloy IN-738LC, *Journal of Materials Processing Technology* 147 (2004) 343-350.
- [3] S.A. Sajjadi, S.M. Zebarjad, Effect of temperature on tensile fracture mechanisms of a Ni-base superalloy, *Archives of Materials Science and Engineering* 28/1 (2007) 34-40.
- [4] S.A. Sajjadi, S.M. Zebarjad, Study of fracture mechanisms of a Ni-Base superalloy at different temperatures, *Journal of Achievements in Materials and Manufacturing Engineering* 18 (2006) 227-230.
- [5] P. Jonsta, Z. Jonsta, J. Sojka, L. Cizek, A. Hernas, Structural characteristics of nickel superalloy Inconel 713LC after heat treatment, *Journal of Achievements in Materials and Manufacturing Engineering* 21/2 (2007) 29-32.
- [6] N.S. Stoloff, Wrought and P/M superalloys, *ASM Handbook, Vol. 1: Properties and Selection Irons, Steels and High-Performance Alloys*, ASM Materials Information Society, 1990, 950-977.
- [7] F. Schubert, Temperature and time dependent transformation: application to heat treatment of high temperature alloys, in: *phase stability in high temperature alloys*, Applied Science Publishers LTD, London, 1981, 119-149.
- [8] Ch.T. Sims, N.S. Stoloff, W.C. Hagel, *Superalloys II*, Ed. A. Wiley Witescience Publications, New York, 1987.
- [9] H. Brandis, B. Huchtemann, *Technologie der Wärmebehandlung warmfeste und hochwarmfester Stähle*, Thyssen Edelst. Techn. Ber. 1 (1981) 28-40 (in German).
- [10] A.K. Koul, J.P. Immarrigeon, W. Wallace, *Microstructural Control in Ni-Base Superalloys*, In: *Advances in High Temperature Structural Materials and Protective Coatings*, National Research Council of Canada, Ottawa, 1994, 95-125.
- [11] P. Bała, New tool materials based on Ni alloys strengthened by intermetallic compounds with a high carbon content, *Archives of Materials Science and Engineering* 42/1 (2010) 5-12.
- [12] P. Bała, Influence of solution heat treatment on the microstructure and hardness of the new Ni-based alloy with a high carbon content, *Archives of Materials Science and Engineering* 45/1 (2010) 40-47.
- [13] M. Zielińska, M. Yavorska, M. Poręba, J. Sieniawski, Thermal properties of cast nickel based superalloys, *Archives of Materials Science and Engineering* 44/1 (2010) 35-38.
- [14] J. Łabanowski, Evaluation of reformer tubes degradation after long term operation, *Journal of Achievements in Materials and Manufacturing Engineering* 43/1 (2010) 244-251.
- [15] K.J. Ducki, M. Hetmańczyk, The influence of prolonged aging on the structure and properties of precipitation hardened austenitic alloy, *Materials Engineering* 4 (2001) 290-293.
- [16] K.J. Ducki, Analysis of the precipitation and growth processes of intermetallic phase in a high-temperature Fe-Ni alloy, *Materials Engineering* 2 (2007) 53-58 (in Polish).
- [17] K.J. Ducki, Structure and precipitation strengthening in a high-temperature Fe-Ni alloy, *Archives of Materials Science and Engineering* 28/4 (2007) 203-210.
- [18] K.J. Ducki, Analysis of the structure and precipitation strengthening in a creep resisting Fe-Ni alloy, *Journal of Achievements in Materials and Manufacturing Engineering* 21/2 (2007) 25-28.
- [19] K.J. Ducki, M. Cieśla, Effect of heat treatment on the structure and fatigue behaviour of austenitic Fe-Ni alloy, *Journal of Achievements in Materials and Manufacturing Engineering* 30/1 (2008) 19-26.
- [20] A. Hernas, *Creep Strength of Steels and Alloys*, Publishing by Silesian University of Technology, Gliwice, 2000 (in Polish).